Hindawi
Advances in Materials Science and Engineering
Volume 2021, Article ID 5567873, 18 pages
https://doi.org/10.1155/2021/5567873

Research Article

Durability Evaluation of Concrete with Multiadmixtures under Salt Freeze-Thaw Cycles Based on Surface Resistivity

Shibin Luo,[1,2] **Wei Liang**,[3] **Hua Wang**,[4,5] **Wensheng Wang**,[1,6] **and Rongjun Zou**[7]

[1]*College of Transportation, Jilin University, Changchun 130025, China*
[2]*Guangxi Hechi Highway Development Center, Hechi 537000, China*
[3]*Guangxi Communications Investment Logistics Development Co., Ltd., Nanning 530029, China*
[4]*Guangxi Beibu Gulf Investment Group Co., Ltd., Nanning 530029, China*
[5]*Guangxi Transportation Science and Technology Group Co., Ltd., Nanning 530007, China*
[6]*College of Construction Engineering, Jilin University, Changchun 130025, China*
[7]*Guangxi Yanglu Expressway Co., Ltd., Nanning 530007, China*

Correspondence should be addressed to Hua Wang; wanghua15@mails.jlu.edu.cn and Wensheng Wang; wangws@jlu.edu.cn

Received 5 February 2021; Accepted 27 May 2021; Published 15 June 2021

Academic Editor: Xiangxiong Kong

According to the climatic characteristics of seasonal frozen area in northeast China, the concrete strength tests, surface resistivity, rapid chloride permeability, and freeze-thaw test under salt solution were carried out to study the influences of mineral admixtures and air content on the conventional properties and salt freeze-thaw resistance of concretes. Then, the correlation analysis of surface resistivity with strength and rapid chloride permeability were further investigated. Subsequently, the changes of cumulative mass loss and relative dynamic elastic modulus varying with salt freeze-thaw cycles were analyzed to study the influences of mineral admixtures and air content on salt freeze-thaw resistance of concrete. The test results showed that fly ash (FA) was not conducive to improve the strength and salt freeze-thaw resistance of concrete. However, blast furnace slag (BFS) and silica fume (SF) could improve the compressive and flexural strength of concrete, in which SF can improve its strength more significantly. Increasing the air content of concrete will lead to the reduction of its compressive strength, and the flexural strength first increased and then decreased. Nevertheless, the addition of air-entrainment agent (AEA) has the best effect on improving the salt freeze-thaw resistance of concrete. Moreover, surface resistivity of concrete has a good exponential function relationship with strength and a good power function relationship with rapid chloride permeability. Therefore, it is of great significance for engineering quality control and quickly and nondestructive testing.

1. Introduction

Due to the high strength, considerable durability, and promising economy, concrete has been one of the most widely used building materials in civil engineering since the 20th century [1–6]. When optimizing mix proportion of concrete in many, if not most engineering construction of China, the trial mix with highest strength is the chosen mix proportion [7–12]. Actually, the durability indexes of concrete deserve the same attention as the strength index, especially when the concrete is working in harsh environment [13–17]. In northeast China, as an example, deicing salt has been invariably used to melt ice and snow on roads for decades [18–20]. Consequently, concrete pavements and bridges suffer from freezing and thawing environment strengthened by salt solution. A large number of cases have shown that the durability of concrete with rosy frost resistance will be greatly reduced when serving in this salt freeze-thaw condition. The presence of salt solutions eventually results in premature spalling of the concrete surface [21, 22], which gives rise to additional maintenance costs every year [23, 24].

In general, air entraining agent (AEA) is undoubtedly the most critical admixture in order to improve the frost resistance of concrete [25, 26]. The addition of air entraining agent brings a large number of tiny, enclosed bubbles inside the concrete. The work of Wellman et al. indicated that these bubbles block the growth of the bodies of ice and the generation of hydraulic pressure as water freezes in capillary cavities, effectively improving the frost resistance of concrete [27]. There are quite a few influential factors impacting air entrainment, in which bubble size and bubble distribution are decisive factors [28–30]. However, it is extremely difficult to obtain the bubble size and distribution in fresh concrete for engineering builders. As a rule, measuring the total air content as a quality control measure of air entrainment is practical [30]. Subsequently, much of research has suggested that the optimal air contents are invariably below 7% when giving consideration to concrete strength, frost resistance, and workability [31]. Recently, super air meter becomes a popular tool for assessing the air void system of fresh concrete. Not only does the total air void content matter, but also the distance between different air bubbles plays an important role in controlling freeze-thaw damage in concrete. Powers indicated that ice growth is restricted and the pore pressure can be readily accommodated by a closely spaced air void system [32]. Yuan et al. used CT to obtain the bubble structure distribution information and proposed the void-to-void distance as a factor to evaluate the freezing-thawing resistance with deicing salt performance of cement concrete [33].

Some environment-friendly mineral admixtures for concrete such as fly ash (FA), blast furnace slag (BFS), and silica fume (SF) are strongly recommended to improve salt freeze-thaw resistance because of their contributions to microstructure of concrete [34, 35]. Studies on mechanism for salt freeze-thaw have suggested that the invasion of chlorides is responsible for damages from salt crystals, high degree of saturation, and additional hydraulic pressure [36, 37]. These damages can be alleviated by rational addition of mineral admixtures, which are pozzolanic and finer than cement, filling pore structure and interfacial transition zone of concrete. Consequently, the chloride penetration coefficient would be reduced significantly [38]. Moreover, the reasonable combination of multimineral admixtures would enable concrete to show better performance than that of single-mineral admixture [39, 40]. For instance, silica fume is better than blast furnace slag in changing the pore structure, and multimineral admixtures would improve the chloride penetration and electrical resistance of concretes [41]. In the case of addition of SF, BFS, and FA at the same time, Sun et al. believed that SF provides main prophase strength amongst these three types of mineral admixtures due to its highly early pozzolanic reaction [42]. Then, BFS begins to develop its pozzolanic effect during transitional period. After 28 days, FA also gradually exhibits its own properties and provides its contributions to the strength of concrete. In terms of improvement of resistance to concrete deteriorating factors, Bapat emphasized that the use of mineral admixtures in concrete is the cheapest alternative [43].

The design strength grade of C40 is sufficient for construction concrete of northeast China in many cases. By contrast, the durability of concrete served in salt-frost environment has been more emphasized heavily recently. When taking the concrete technical factors such as design requirements, construction methods, times, and strength grade into consideration, the high-performance concrete might not be suitable for adoption. Accordingly, the air-entrained concrete with multimineral admixtures would be an overwhelmingly feasible and economical choice to improve the resistance of concrete to salt-frost erosion. However, when using the conventional method to design the mix proportion of air-entrained concrete with multimineral admixtures, a large number of trial mixes are required to select the desired combination of materials that meets special performance, which would be costly, time-consuming, and sometimes uneconomical and wasteful [44, 45]. From these considerations, a simple genetic algorithm was applied to optimize the mix proportion design of this multiconstituent concrete in this paper. The genetic algorithm is a global optimizing method which imitates biological evolution and has an advantage over many other methods on handling multiple objectives [46]. Actually, the fitness functions of different indices such as strength, slump, and material price or else have been adopted by researchers in order to obtain optimum mix proportions for target concrete properties through the genetic algorithm [47, 48]. In this paper, aiming at improving the resistance of concrete to salt-frost erosion, the mix proportion of air-entrained concrete with multimineral admixtures was designed based on the genetic algorithm, in which the fitness functions of salt freeze-thaw resistance indices were adopted.

This paper studied the influences of different mineral admixtures and air contents on the performances of concrete. At the same time, the correlation analysis between mechanical properties and durability of concrete was studied. Several groups of concrete specimens with different mineral admixtures (FA, BFS, and SF) and air contents were designed after determining the water binder ratio, cement dosage, sand ratio, and aggregate dosage. Then, the mechanical properties, physical properties, and salt freeze-thaw resistance of concrete specimens were tested. Subsequently, the influences of mineral admixtures on the mechanical and physical properties as well as surface resistivity of concrete were studied, and the quantitative relationship between strength as well as rapid chloride permeability and surface resistivity of concrete were established.

2. Materials and Methods

2.1. Mixture Materials. The ordinary Portland cement (OPC) was procured from Jilin Yatai Dinglu Cement Ltd., and the corresponding grade is P.O. 42.5. To achieve the reasonable application of mineral admixtures and AEA in concrete, FA, BFS, SF, and AEA were introduced into cement concrete for a better salt freeze-thaw resistance [49–52]. The main chemical compositions of OPC, FA, BFS, and SF are shown in Figure 1. In this study, AEA was triterpenoid saponin AEA with the type of SJ-2 to achieve

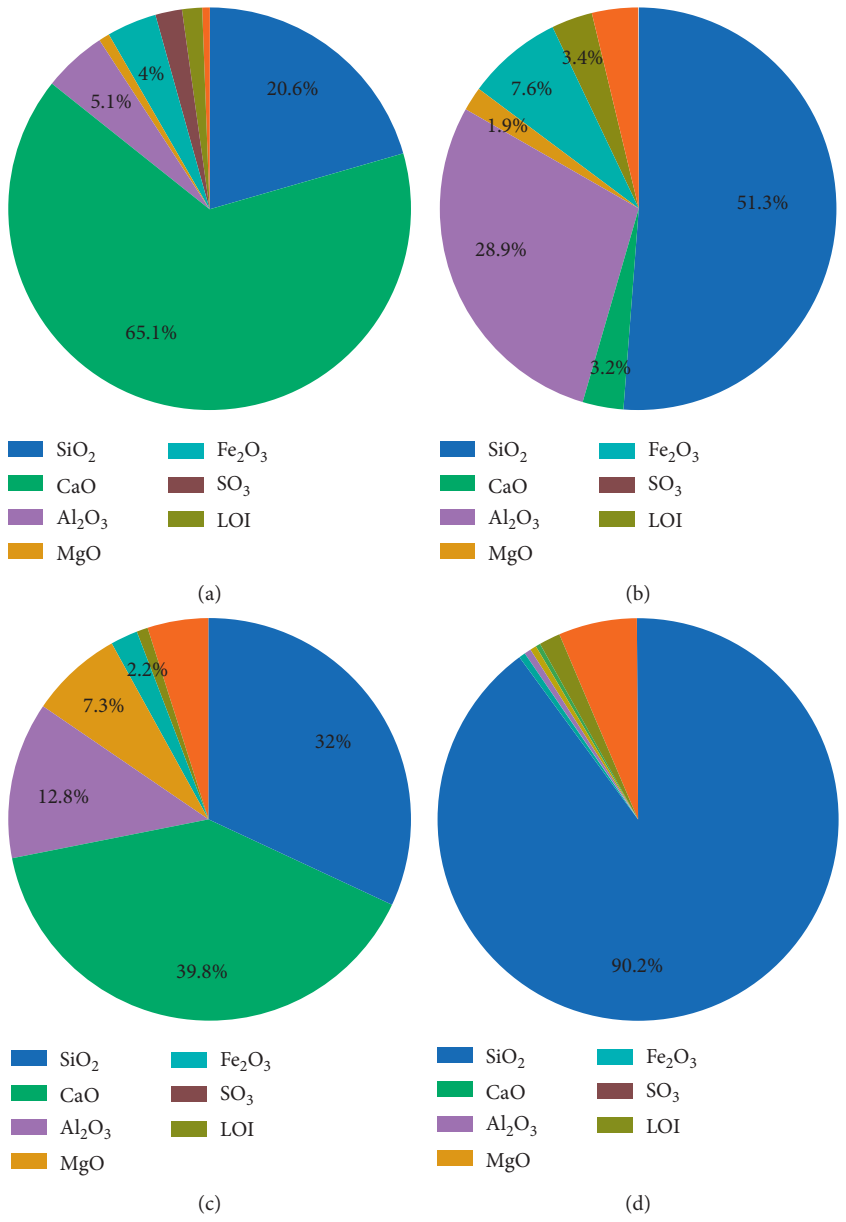

Figure 1: Chemical composition results of binders: (a) OPC. (b) FA. (c) BFS. (d) SF.

different air contents in cement concrete. And naphthalene superplasticizer was also introduced into trial concrete mixes to keep consistent workability, of which the pH value is in the range of 7–9. Following the existing study [53], natural sand with a maximum size of 9.5 mm was used as coarse aggregate and well-graded river sand with a fineness modulus of 2.0 was used as fine aggregates, which were obtained from Jilin Province, China. The specific gravities for natural gravel and river sand are 2.76 and 2.64, respectively.

2.2. Mixture Proportion and Specimen Preparation. In order to analyse the influences of FA, BFS, SF, and AEA on the salt freeze-thaw resistance of cement concretes, different dosages of AEA and several mineral admixtures were studied. The dosage of FA or BFS should be controlled within 30% by the total mass of cementitious materials, respectively [54–56]. Meanwhile, the total dosage of FA and BFS was limited to less than 40% by the total mass of cementitious materials. By contrast, the dosage of SF was controlled not to exceed 10% due to its high activity and cost. Besides, considering that the influence of AEA on the frost resistance of concrete is higher than that of multimineral admixtures [31], the AEA content was designed and divided into three feasible range levels of air content, i.e., $(2.5 \pm 0.5)\%$, $(4.5 \pm 0.5)\%$, and $(6.5 \pm 0.5)\%$.

Following the above mixture proportion ranges, a total of 15 groups of concrete proportions with various dosages and combinations of FA, BFS, SF, and AEA were prepared for the concretes used in this study. In the mixture design, OPC, FA, BFS, and SF were used as the main components of binders and the total binder content in all concrete

specimens was kept constant at 423 kg/m^3. A target concrete strength grade of C40 was selected for pavement concrete mixtures, and the water-to-binder ratio of all these cement concretes was also kept constant at 0.40. After that, a concrete mixer was applied to mix all the raw materials, and naphthalene superplasticizer was carefully added to the mixture to maintain a slump range of (45 ± 5) mm. The air content range levels in concrete specimens were controlled by AEA with the type of SJ-2 in accordance with the Chinese specification JTG E30-2005. These 15 groups of mixture proportions with various dosages of FA, BFS, SF, and AEA, including single admixture, double admixtures, and triple admixtures, are shown in Table 1. The dosage of AEA is characterized by the air content. Three dosage levels of FA, BFS, SF, and AEA of concrete specimens were determined and applied, for example, FA-10 means replacing 10% of OPC with FA and AEA-2 means air content of (2.5 ± 0.5)%.

Referring to the Chinese specification JTG E30-2005 and existing literature [1, 57, 58], three types of cement concretes were selected and prepared in this paper, in which specimens with 100 mm × 100 mm × 100 mm were used for the 28-day compression test, specimens with 100 mm × 100 mm × 400 mm were used for the 28-day flexural test, and specimens with 40 mm × 40 mm × 160 mm were used for the surface resistivity test and salt freeze-thaw cycle test. For each type of geometric dimensions, the number of each mixture proportion for these 15 groups of cement concretes was determined as three, i.e., three replicate specimens. In accordance with the related specification, after the preparation was completed, all the concrete specimens were firstly placed in the standard curing room with a temperature of 20°C and relative humidity of 95% for 24 h of sealed curing and then demoulded. These concrete specimens will continue to be placed in the standard curing room for 27 days.

2.3. Experimental Methods

2.3.1. Compressive Strength Test and Flexural Strength Test. The compressive strength and flexural strength at the age of 28 days were tested according to ASTM C39/C39M-18. The specimen sizes of compressive strength test and flexural strength test were described in the above section, and the universal testing machine was performed on three replicate specimens for the mechanical tests, as shown in Figure 2. For the compressive strength test, the loading rate was set as 0.5 MPa/s. For the flexural strength test, the loading rate was set as 0.05 MPa/s. During the whole process of test loading, the load and deflection of the specimens were recorded in real time. Then, the corresponding compressive strength (S_c) and flexural strength (S_f) could be calculated.

2.3.2. Surface Resistivity Test and Rapid Chloride Permeability Test. The four-probe method is used to determine the surface resistivity of concrete specimens. In this paper, the Resitest-400 instrument was adopted to measure the surface resistivity of concrete specimens after 28 days of curing. Before testing, the saturated sponge was put into the sensors, which were connected to the host through a cable. The surface resistivity test is shown in Figure 3(a).

The rapid chloride permeability test of cement concrete was carried out to evaluate the resistance to chloride ion penetration of concrete according to ASTM C1202. These specimens of rapid chloride permeability test were 100 mm in diameter and 50 mm in height. The side surfaces of all specimens were firstly coated with rapid setting epoxy. These specimens were placed inside an automatic vacuum water-soaking machine to saturate for 18 hours, and then the electrical fluxes of concrete specimens were determined. The setups of the surface resistivity test and rapid chloride permeability test are illustrated in Figure 3(b).

2.3.3. Salt Freeze-Thaw Cycle Test. In the salt freeze-thaw cycles, the concrete specimens with size of 40 mm × 40 mm × 160 mm were immersed in 3% concentration salt solution and exposed to freeze-thaw condition at the same time. A special freeze-thaw machine was adopted to create temperature conditions, as shown in Figure 4. The duration of one freeze-thaw cycle was 12 hours, in which the lowest and highest temperatures were −18°C and 18°C, respectively. The freeze-thaw test was terminated when any specimen showed considerable surface damage or reduction in relative dynamic modulus of elasticity value of more than 80% of the initial value [23]. After multiple salt freeze-thaw cycles, the mass of concrete specimens and ultrasonic propagation speeds in specimens were also measured, as shown in Figure 4. Then, the mass loss (M_n) and variation of relative dynamic elasticity modulus (R_n) of specimens can be calculated by using equations (1) and (2), respectively:

$$M_n = \frac{m_0 - m_n}{m_0} \times 100\%, \quad (1)$$

where m_0 is the initial mass of concrete specimens before exposed to salt freeze-thaw condition and m_n is the mass of concrete specimens after n salt freeze-thaw cycles:

$$R_n = \frac{(v_n)^2}{(v_0)^2} \times 100\%, \quad (2)$$

where v_0 is the ultrasonic propagation speed in specimens before exposed to salt freeze-thaw condition and v_n is the ultrasonic propagation speed in specimens after n salt freeze-thaw cycles.

3. Results and Discussion

3.1. Influence Analysis of Mineral Admixtures and Air Content on Physical and Mechanical Performances of Concretes

3.1.1. Influence of Single-Mineral Admixture-FA. The 28-day compressive strength, flexural strength, surface resistivity, and rapid chloride permeability of concretes with FA are shown in Figure 5. It can be seen from Figure 5(a) that the 28-day compressive strength of control cement concrete is 42.9 MPa. With the increase of FA content, the compressive strength of cement concrete decreases, and FA has a great influence on the compressive strength of concrete, as

Table 1: Mix proportions of concretes with multiadmixtures (kg/m^3).

No.	OPC	FA	BFS	SF	Air content (%)	Fine aggregate	Coarse aggregate	Slump (mm)
Control	423	—	—	—	1	584	1240	45 ± 5
FA-10	381	42	—	—	1	584	1240	45 ± 5
FA-20	338	85	—	—	1	584	1240	45 ± 5
FA-30	296	127	—	—	1	584	1240	45 ± 5
BFS-10	381	—	42	—	1	584	1240	45 ± 5
BFS-20	338	—	85	—	1	584	1240	45 ± 5
BFS-30	296	—	127	—	1	584	1240	45 ± 5
SF-3	410	—	—	13	1	584	1240	45 ± 5
SF-6	398	—	—	25	1	584	1240	45 ± 5
SF-9	385	—	—	38	1	584	1240	45 ± 5
FA-BFS	296	63.5	63.5	—	1	584	1240	45 ± 5
FA-BF-BFS	271	63.5	63.5	25	1	584	1240	45 ± 5
AEA-2	423	—	—	—	2.5	584	1240	45 ± 5
AEA-4	423	—	—	—	4.5	584	1240	45 ± 5
AEA-6	423	—	—	—	6.5	584	1240	45 ± 5

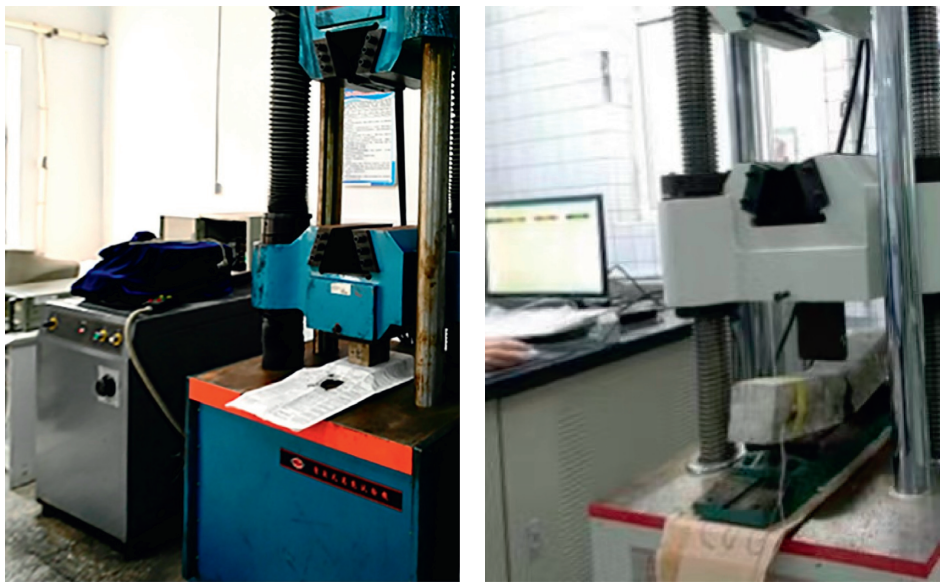

(a) (b)

Figure 2: Mechanical performance tests of cement concretes used in this paper. (a) Compressive strength test. (b) Flexural strength test.

concluded by Mardani-Aghabaglou et al. [51]. When the FA content is 30%, the strength decreases to 34.69 MPa. From Figure 5(b), it can be seen that the 28-day flexural strength of control cement concrete is 4.95 MPa, and the flexural strength of cement concrete is 4.48 MPa, 4.25 MPa, and 3.92 MPa when the FA contents are 10%, 20%, and 30%, which indicates that the flexural strength of cement concrete decreases with the increase of FA content, which is line with the findings of Mardani-Aghabaglou et al. [51]. It can be seen from Figure 5(c) that the surface resistivity increases with the increase of FA content, and the surface resistivity changes slightly with the increase of FA content in the range of 10%~20%, as previously described in [59]. In Figure 5(d), the rapid chloride permeability of control cement concrete in 28 days is 1951.5 C. With the increase of FA content, the rapid chloride permeability decreases. When the FA content is 10%, 20%, and 30%, the rapid chloride permeability of concrete is 1297.5 C, 1192.5 C, and 972.5 C, respectively. When the FA content is within 0%~10%, the rapid chloride permeability decreases the most. When the FA content is higher than 10%, the reduction range of rapid chloride permeability becomes smaller, which indicates that the appropriate content of FA can effectively reduce the rapid chloride permeability of concrete [59].

The mechanical properties of concrete with FA decrease with the increase of FA content, and the decrease range increases with the increase of FA content, which indicates that the secondary hydration degree of FA is low in the 28-day strength formation process, which is not enough to improve the strength of concrete [35]. The surface resistivity

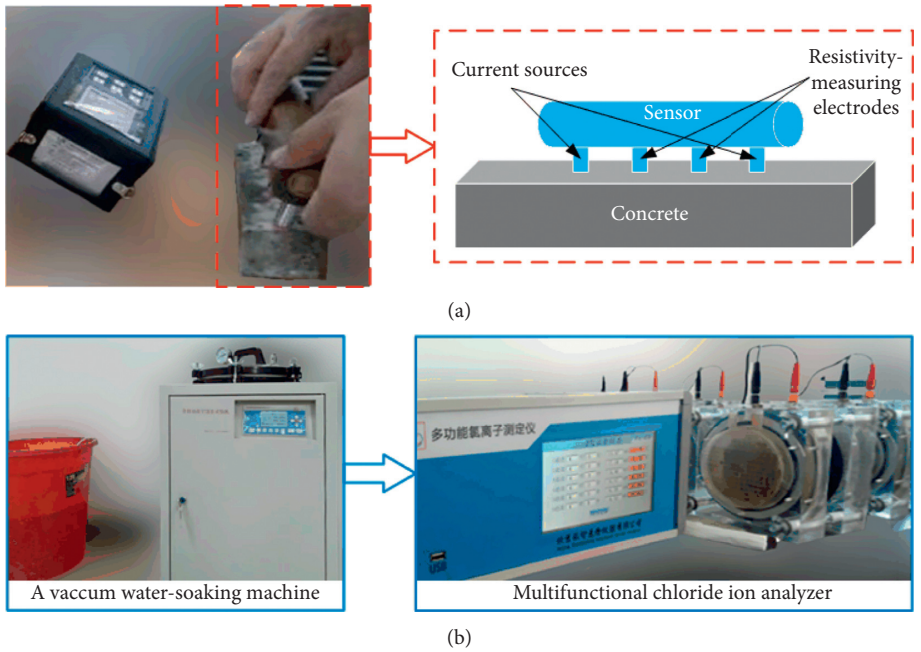

Figure 3: Surface resistivity test and rapid chloride permeability test of cement concretes. (a) Surface resistivity test. (b) Rapid chloride permeability test.

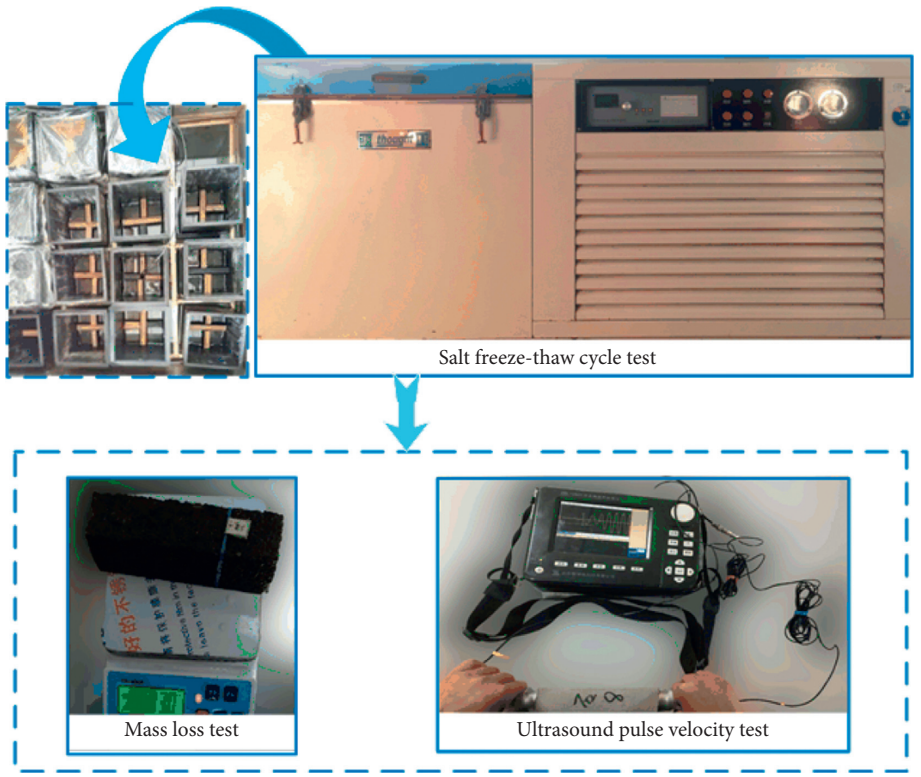

Figure 4: Salt freeze-thaw cycle test of cement concretes.

of concrete increases with the increase of FA content. The electric flux of concrete decreases with the increase of fly ash content. The rapid chloride permeability reflects the chloride penetration resistance of concrete. The higher the rapid chloride permeability, the stronger the chloride ion resistance of concrete. From the surface resistivity and rapid chloride permeability of concrete added with FA, the compactness of concrete has been improved, mainly because

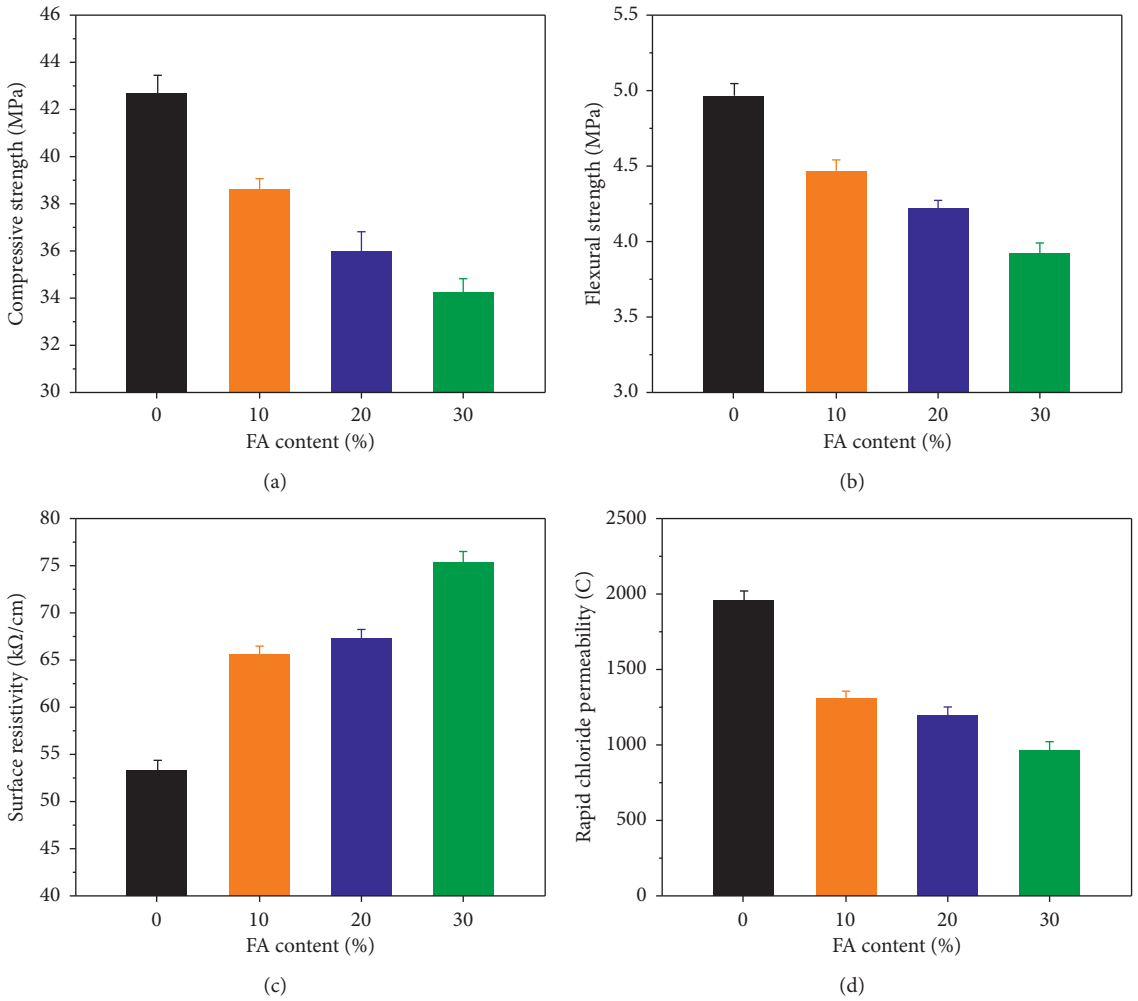

Figure 5: Influence of single-mineral admixture-FA on the performances of concrete. (a) Compressive strength. (b) Flexural strength. (c) Surface resistivity. (d) Rapid chloride permeability.

FA plays the role of microaggregate filling, which can fill the internal defects of concrete [49]. Therefore, the surface resistivity and rapid chloride permeability of concrete are improved.

3.1.2. Influence of Single-Mineral Admixture-BFS. The influences of BFS contents on 28-day compressive strength, flexural strength, surface resistivity, and rapid chloride permeability of concrete are shown in Figure 6.

It can be seen from Figure 6(a) that the compressive strength of cement concrete increases with the increase of BFS content in the range of 0%~30%, the compressive strength of concrete increases slowly in the range of 0%~20%, and the compressive strength of concrete increases faster in the range of 20%~30%. When the BFS content is 30%, the compressive strength of concrete is 47.26 MPa. It can be seen from Figure 6(b) that with the increase of BFS content, the flexural strength of concrete increases, and the flexural strength of concrete increases linearly with BFS content. When BFS content is 30%, the flexural strength is 6.05 MPa. The test results indicate that compressive strength and flexural strength are consistent with previous study [43, 59, 60]. From Figure 6(c), it can be seen that the surface resistivity of concrete increases fastest when the BFS content is 0%~10% and slows down when the BFS content is 10%~30%, which indicates that adding a small amount of BFS can improve the surface resistivity of concrete [59]. It can be seen from Figure 6(d) that the rapid chloride permeability of cement concrete decreases linearly with the increase of BFS content in the content range of 0%~30%. When the BFS content is 30%, the rapid chloride permeability is 950.5 C.

In the case of single-mineral admixture-BFS, the mechanical properties of concrete increase with the increase of BFS content, the surface resistivity increases with the

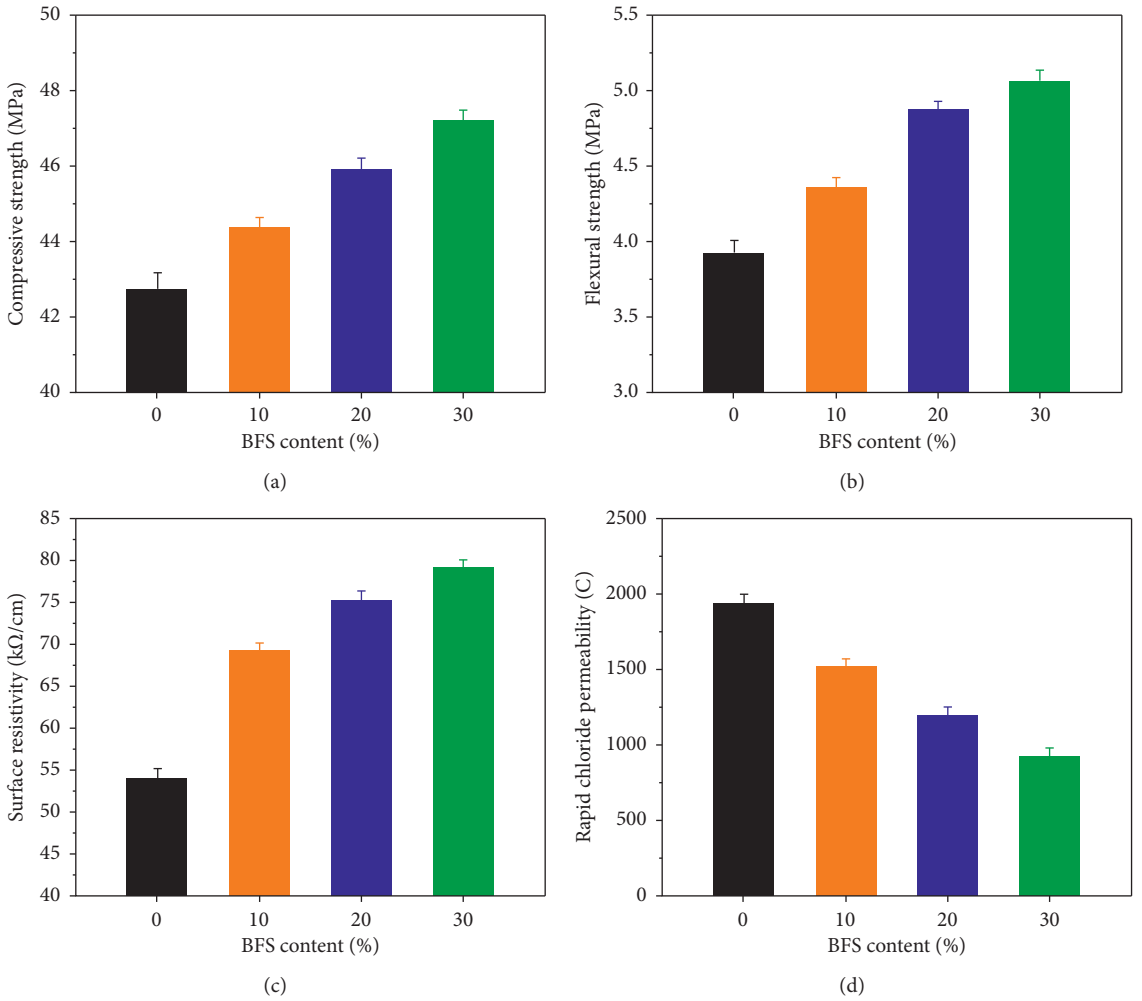

Figure 6: Influence of single-mineral admixture-BFS on the performances of concrete. (a) Compressive strength. (b) Flexural strength. (c) Surface resistivity. (d) Rapid chloride permeability.

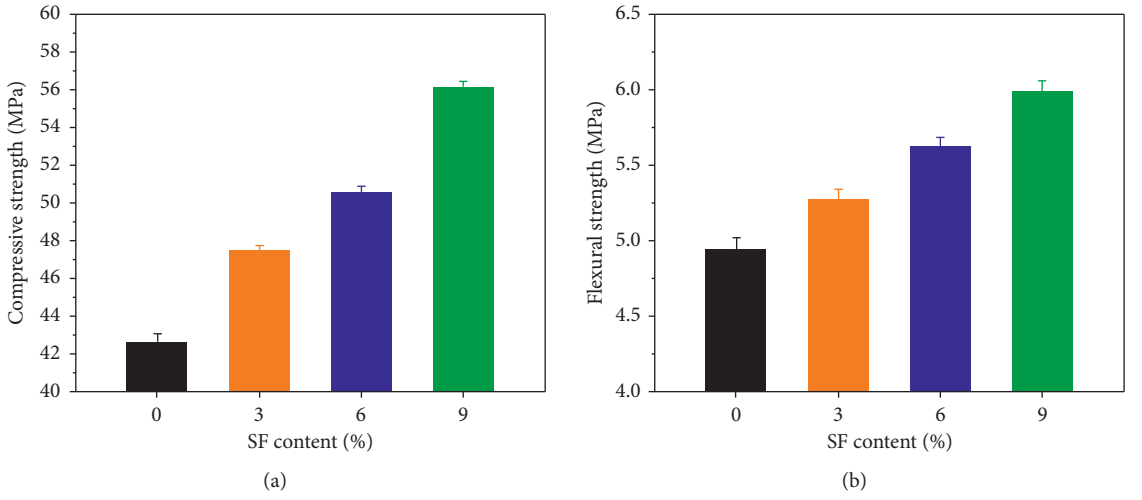

Figure 7: Continued.

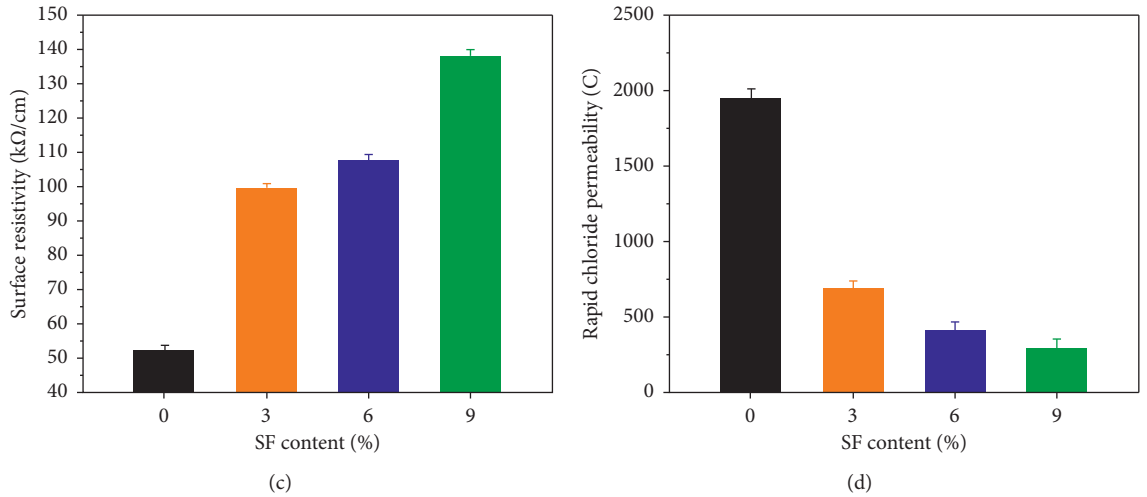

Figure 7: Influence of single-mineral admixture-SF on the performances of concrete. (a) Compressive strength. (b) Flexural strength. (c) Surface resistivity. (d) Rapid chloride permeability.

increase of BFS content, and the rapid chloride permeability decreases with the increase of BFS content. BFS contains a lot of oxides (such as Al_2O_3 and CaO), which has high activity in hydration [60]. It can be hydrated more in 28 days to improve the strength of concrete. At the same time, the physical properties of concrete are improved due to the filling effect of microaggregate and secondary hydration.

3.1.3. Influence of Single-Mineral Admixture-SF. The influences of SF content on 28-day compressive strength, flexural strength, surface resistivity, and rapid chloride permeability of concrete are shown in Figure 7.

It can be seen from Figure 7(a) that when the SF content is in the range of 0~9%, the concrete strength increases with the increase of SF content, and the concrete strength increases linearly with the SF content. When the SF content is 9%, the concrete strength can reach 56.47 MPa. It can be seen from Figure 7(b) that the flexural strength of concrete increases with the increase of SF content. When the SF content is 6%, the flexural strength of concrete has a maximum value. The strength results are consistent with the analysis results [50, 51, 59]. It can be seen from Figure 7(c) that with the increase of SF content, the surface resistivity of concrete increases. When the SF content is 9%, the resistivity of concrete can reach 137.3 kΩ/cm. It can be seen from Figure 7(d) that the rapid chloride permeability of concrete decreases exponentially with the addition of SF, which indicates that the rapid chloride permeability of concrete can be greatly reduced by adding a small amount of SF.

SF contains more than 90% of silica. In the alkaline environment formed after cement hydration, the secondary hydration degree of SF is larger [50]. In addition, the fineness of SF is larger and the microaggregate is filled more fully, which improves the mechanical and physical properties of concrete.

3.1.4. Influence of Multimineral Admixtures. The influences of multimineral admixtures on 28-day compressive strength, flexural strength, surface resistivity, and rapid chloride permeability of concrete are shown in Figure 8.

It can be seen from Figure 8(a) that when the content of FA and BFS is 15%, respectively, the compressive strength of concrete is 45.83 MPa. Under the same proportion of FA and BFS, adding 6% SF, the strength can reach 48.02 MPa. It can be seen from Figure 8(b) that when the content of FA and BFS is 15% respectively, the flexural strength of concrete is 5.46 MPa. Under the same proportion of FA and BFS, adding 6% SF, the strength can reach 5.86 MPa. It can be seen from Figure 8(c) that the surface resistivity of double admixtures is 86.05 kΩ/cm, while that of triple admixtures is 119.35 kΩ/cm, which indicates that SF can effectively improve the resistivity of concrete. It can be seen from Figure 8(d) that the rapid chloride permeability of concrete can be effectively reduced in the case of double mixing, but when 6% SF is added, the rapid chloride permeability is only 287.5 C, which indicates that SF can effectively reduce the rapid chloride permeability of concrete. This is similar to the previous research results [39, 43, 59].

The results showed that the mechanical properties of the concrete are better than that of the control cement concrete, which indicates that the hydration and secondary hydration of mineral admixtures are sufficient in the process of strength formation, which can provide strength for the concrete [1, 34, 58].

3.1.5. Influence of Air Contents by AEA. The influences of air contents on 28-day compressive strength, flexural strength, surface resistivity, and rapid chloride permeability of concrete are shown in Figure 9.

It can be seen from Figure 9(a) that the compressive strength of concrete decreases with the increase of air content. When the air content is 2.5%, the compressive strength of concrete is 37.88 MPa. When the air content is 6.5%, the compressive strength of concrete is only 30.6 MPa. It can be seen from Figure 9(b) that with the increase of air

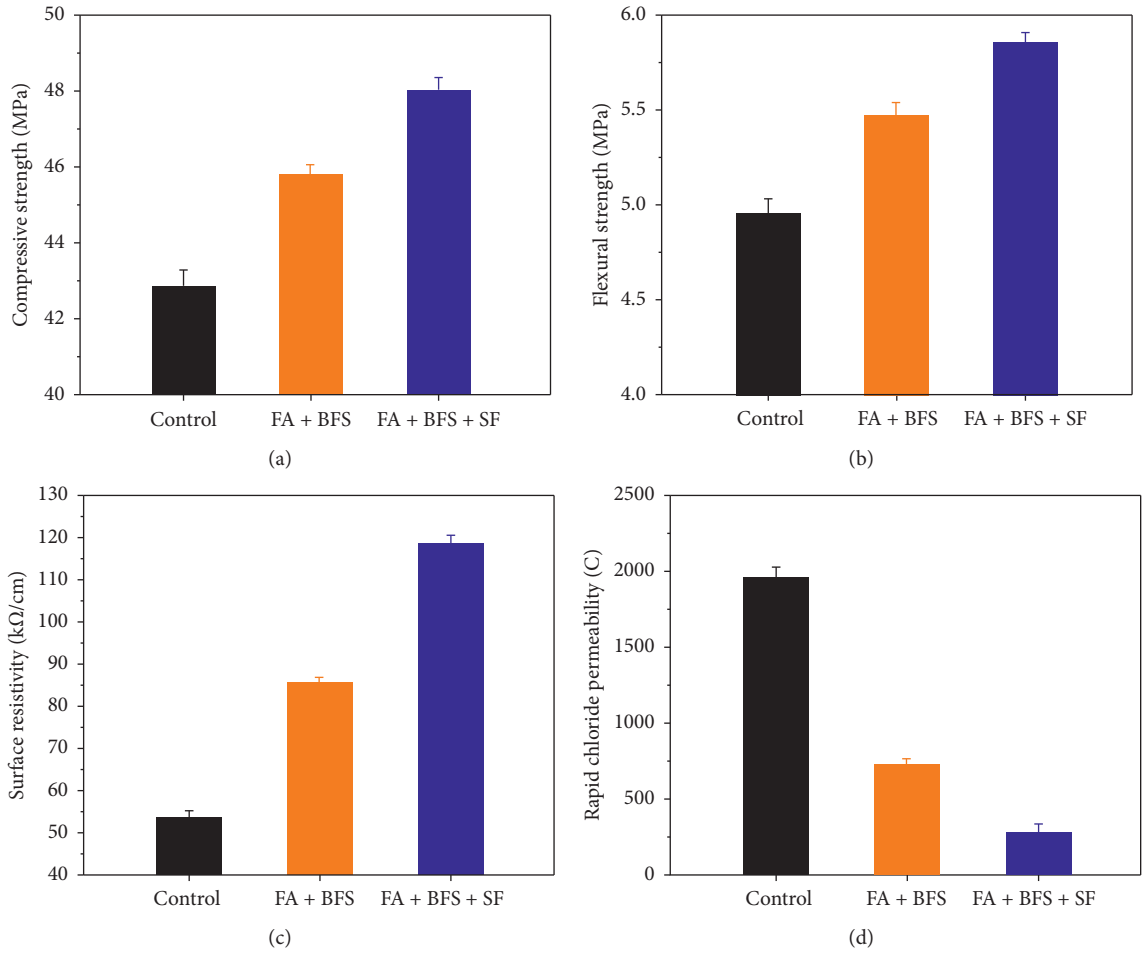

Figure 8: Influence of multimineral admixtures on the performances of concrete. (a) Compressive strength. (b) Flexural strength. (c) Surface resistivity. (d) Rapid chloride permeability.

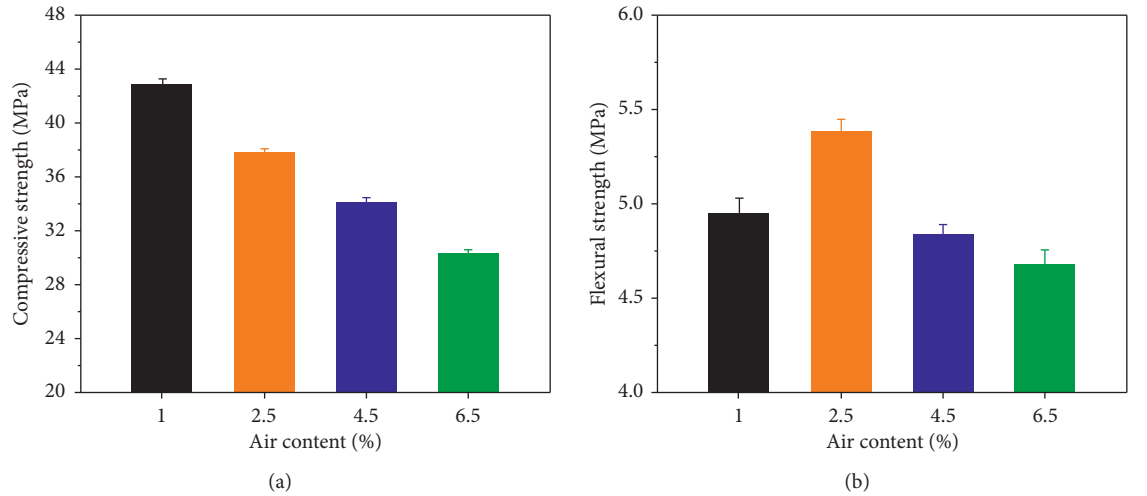

Figure 9: Continued.

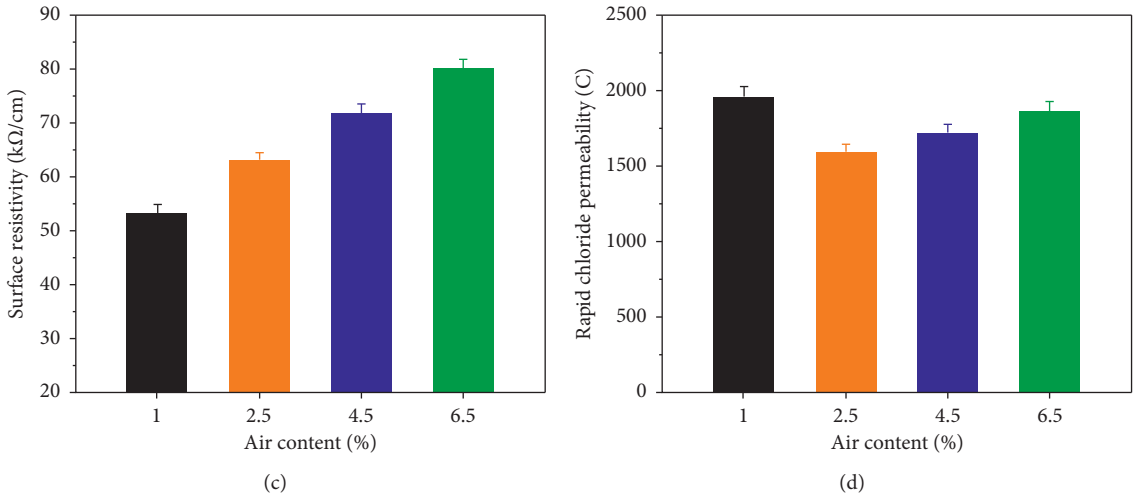

Figure 9: Influence of air contents on the performances of concrete. (a) Compressive strength. (b) Flexural strength. (c) Surface resistivity. (d) Rapid chloride permeability.

content in the range of 1%~6.5%, the flexural strength first increases and then decreases, and there is a maximum value of flexural strength, that is, when the air content is 2.5%, the maximum flexural strength of cement concrete is 5.38 MPa, as previously described in [25]. It can be seen from Figure 9(c) that the surface resistivity of concrete increases with the increase of air content. When the air content is 6.5%, the maximum value of concrete resistivity is 79.35 kΩ/cm. It can be seen from Figure 9(d) that the rapid chloride permeability of concrete decreases with the increase of air content in the air content range of 1%~2.5% and increases with the increase of air content in the air content range of 2.5%~6.5%. When the air content is 2.5%, the minimum rapid chloride permeability of concrete is 1596 C, which is line with the findings of Li et al. [59].

With the increase of air content, the air in concrete increases, and the compressive strength of concrete decreases. The rapid chloride permeability of concrete first decreases and then increases with the increase of air content. This is because with the increase of air content, tiny closed bubbles are formed in concrete, and the capillary channels in concrete are destroyed [2, 31].

3.2. Correlation Analysis between Surface Resistivity and Mechanical and Rapid Chloride Permeability Properties

3.2.1. Correlation Analysis between Surface Resistivity and Compressive and Flexural Strength. Concrete strength is a comprehensive index to measure the quality of concrete [4]. Concrete resistivity is an important electrochemical parameter of concrete, which can be used to characterize the internal microstructure of concrete and evaluate the permeability of concrete [50]. If the quantitative relationship between concrete compressive strength and resistivity can be established, the development trend of concrete compressive strength can be inferred by concrete resistivity, and vice versa. The relation curves between surface resistivity and strength of concrete (i.e., compressive and flexural strength) are shown in Figure 10.

For single-mineral admixture-FA, the surface resistivity of concrete is negatively correlated with compressive strength and flexural strength [59]. With the increase of strength (compressive and flexural), the surface resistivity decreases gradually. The parameter relationships have good nonlinear correlations, and the correlation coefficients are greater than 0.94. For single-mineral admixture-BFS or SF, the surface resistivity of concrete is positively correlated with compressive strength and flexural strength [49]. With the increase of strength (compressive and flexural), the surface resistivity increases gradually. The parameter relationships have good nonlinear correlations, and the correlation coefficients are greater than 0.93. While in the case of multiple admixtures, the surface resistivity of concrete is still positively correlated with the compressive strength and flexural strength. With the increase of strength, the resistivity increases gradually. The parameter relationship has a good nonlinear correlation, and the correlation coefficients are greater than 0.98. The compressive and flexural strength of concrete with FA would decrease with the increase of surface resistivity; however, the compressive and flexural strength of concrete with BFS, SF, or multimineral admixture would increase with the increase of surface resistivity, i.e., strength $= a \times e^{bx}$. At the same time, it also shows that adding FA instead of cement, the early strength of concrete gradually decreases, and BFS and SF are conducive to the improvement of the early strength of concrete [50, 60]. For the air content, the compressive and flexural strength of concrete change with the increase of surface resistivity in a polynomial power function.

According to the test results, the development trend of concrete strength can be predicted. The surface resistivity of concrete can not only reflect the density and pore structure of concrete statically but also indirectly reflect the correlation between strength and density.

3.2.2. Correlation Analysis between Surface Resistivity and Rapid Chloride Permeability. The four-probe method used

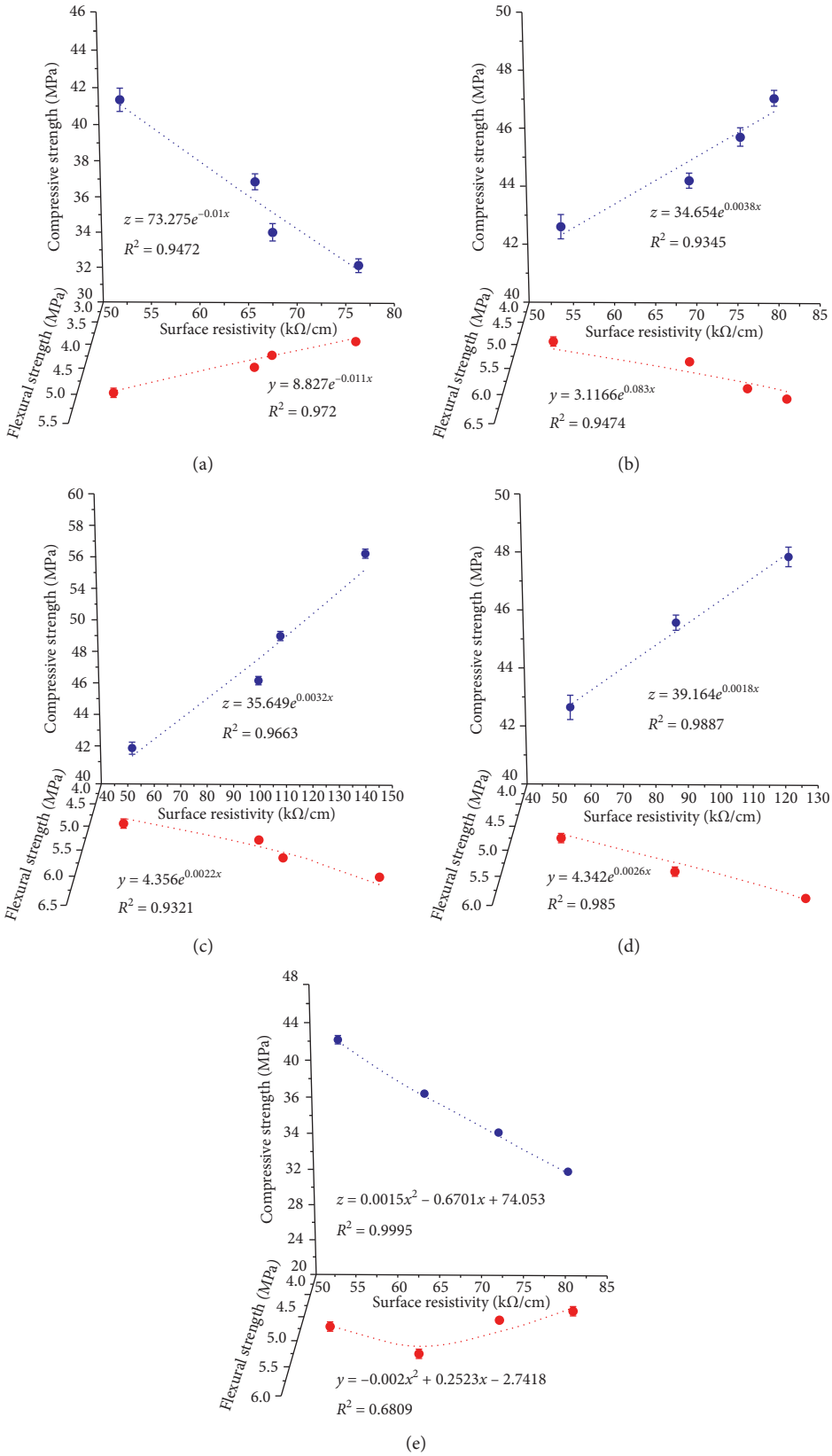

Figure 10: Correlation analysis between surface resistivity and mechanical properties. (a) FA. (b) BFS. (c) SF. (d) Multimineral admixtures. (e) Air contents.

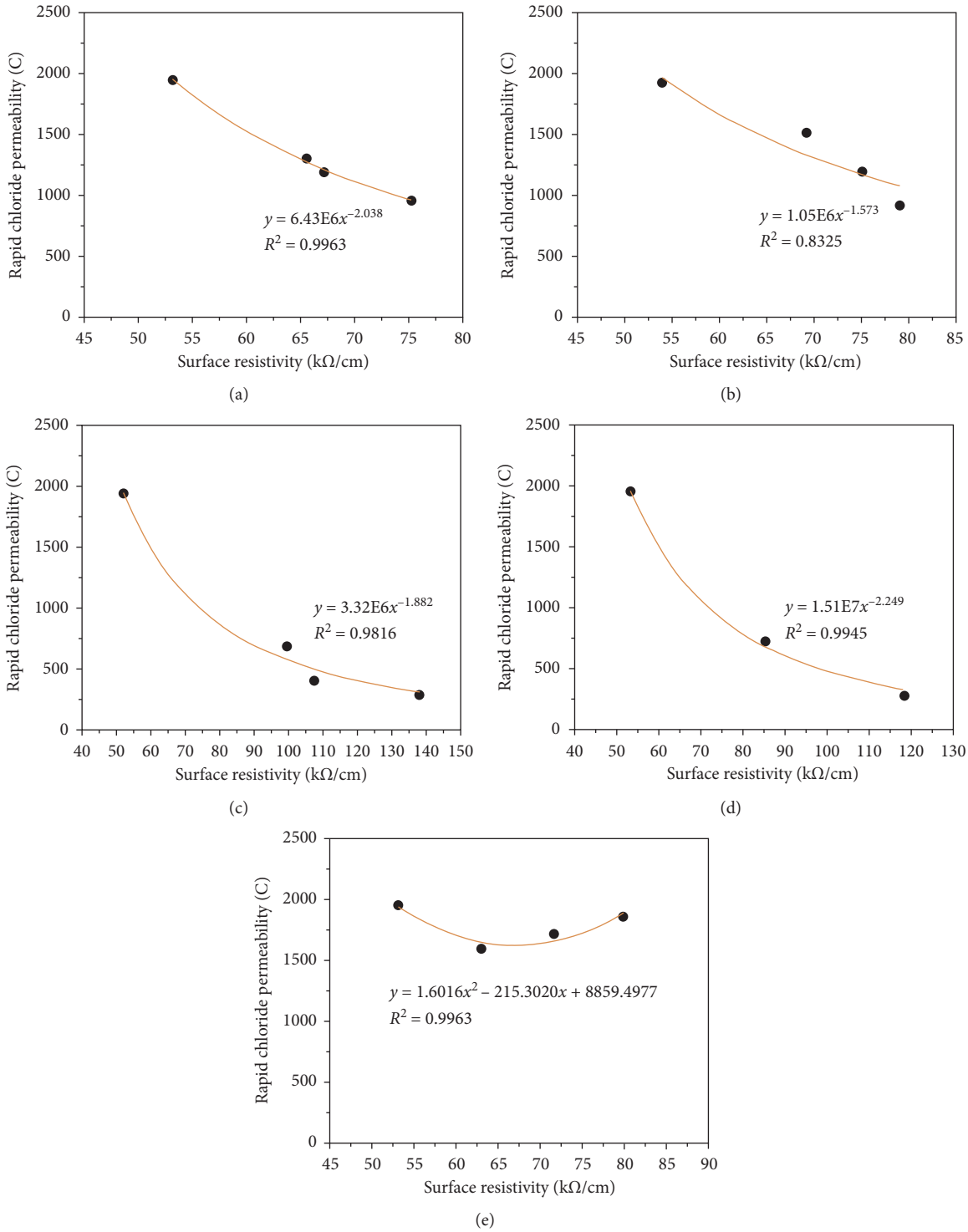

Figure 11: Correlation analysis between surface resistivity and rapid chloride permeability. (a) FA. (b) BFS. (c) SF. (d) Multimineral admixtures. (e) Air contents.

to test the surface resistivity of concrete and the rapid chloride permeability method used to test the chloride ion penetration resistance of concrete are both electrical test methods [59]. Both methods could reflect the compactness of concrete, so these two test results can be fitted and analyzed. The results are shown in Figure 11. It can be seen from Figure 11 that when power function regression is adopted, the correlation coefficient between rapid chloride permeability and surface resistivity reaches around 0.9, which shows that they have a good correlation.

Concrete is a kind of porous medium [33, 41]. There are many kinds of conductive ions in its pore solution, which

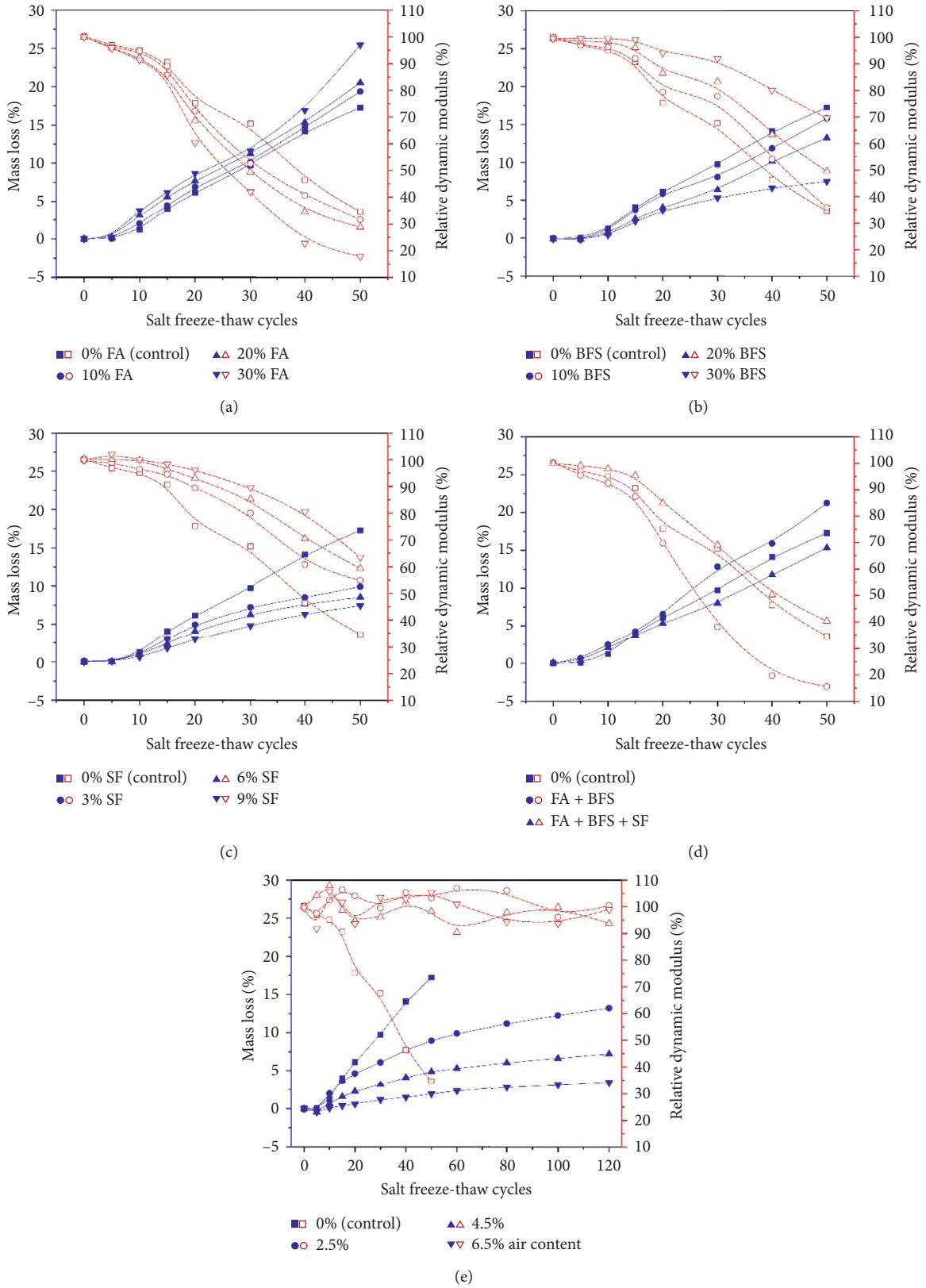

Figure 12: The salt freeze-thaw resistance of concretes with mineral admixtures. (a) FA. (b) BFS. (c) SF. (d) Multimineral admixtures. (e) Air contents.

have great influence on the conductivity of concrete. No matter the rapid chloride permeability method or the four-probe method, it is necessary to apply voltage on the specimen to measure the electric quantity of the corresponding part. The difference is that the rapid chloride permeability method tests the total electric quantity passing through the axial direction of the cylinder specimen, while the four-probe method tests the surface resistivity of the cylinder specimen with a depth of about 30 mm [59]. The two methods are similar but different, and the conversion relationship between them can be obtained by regression analysis. Compared with the rapid chloride permeability method, the surface resistivity test method does not need to cut and keep water, which has the advantages of saving time and labor, and has the potential of popularization and application.

3.3. Evaluation of Salt Freeze-Thaw Resistance of Concretes with Mineral Admixtures. Compared with the control group, the cumulative mass loss, and relative dynamic modulus of elasticity of concrete with different single, multiple and air content under salt freeze-thaw cycles are shown in Figure 12.

From Figure 12(a), it can be seen that in the first five salt freeze-thaw cycles, the mass loss of concrete with FA showed negative numbers. After that, the mass loss of the four concretes increased with the increase of salt freeze-thaw cycles. This shows that in the early stage of salt freeze-thaw, because the pores in the concrete were not completely saturated during the immersion period, the ice crystal pressure forced the intrusion of salt water during the freeze-thaw process [22, 57, 58]. At this time, the mass loss of concrete during the salt freeze-thaw process was less than the mass of the invading salt water. When the intruding salt water reaches a state of equilibrium and the mass of the intruding salt water reaches relative saturation, the concrete will experience mass loss, and the situation will occur after 5 salt freeze-thaw cycles. In addition, with the increase of FA content, the mass loss of concrete is greater. With respect to relative dynamic modulus, as the salt freeze-thaw cycle increases, the relative dynamic modulus of concrete decreases. In the first 15 salt freeze-thaw cycles, the relative dynamic modulus of concrete has a small decrease, and the freeze-thaw effects are consistent. The variation of mass loss and relative dynamic modulus with FA has been described in previous publications [50, 51]. When there are more than 15 salt freeze-thaw cycles, the relative dynamic modulus of concretes decreased greatly. With the increase of FA content, the relative dynamic modulus of concrete decreases more greatly. Therefore, with the increase of FA content, the salt freeze-thaw resistance of concrete decreases, as reported by Liu et al. [35].

It can be seen from Figure 12(b) that the mass loss of concrete with BFS increases with the increase of salt freeze-thaw cycles, but in the first 5 salt freeze-thaw processes, the mass loss of concrete decreases with the increase of salt freeze-thaw cycles, and the principle is described above. In the process of the salt freeze-thaw cycle, the mass loss of concrete decreases with the increase of BFS content. In addition, with the increase of salt freeze-thaw cycles, the relative dynamic modulus of concrete decreases. In the BFS content range of 0%~30%, the greater the BFS content, the better the salt freeze-thaw resistance of concrete. This may be due to the high activity of BFS, which contains more oxides, hydration in water, and secondary hydration in alkaline environment will form cementitious substances. At the same time, due to the filling effect of micro-aggregate, the salt freeze-thaw resistance of concrete is improved [60].

In Figure 12(c), it can be seen that the mass loss of concrete increases with the increase of salt freeze-thaw cycles. When the SF content is in the range of 3%~6%, the mass loss trend is the same, which indicates that a small amount of SF can reduce the mass loss of concrete. At the same time, with the increase of salt freeze-thaw cycles, the relative dynamic modulus of concrete decreases. The reason may be that SF contains a lot of silica, in the secondary hydration, there is more silica hydration, and at the same time, due to the filling effect of microaggregate [61], the salt freeze-thaw resistance of concrete is improved.

It can be seen from Figure 12(d) that the mass loss of FA and BFS compound concrete under salt freeze-thaw cycles is not improved compared with that of control concrete, but the spalling resistance is decreased. However, when 6% SF was added, that is, in the case of three mineral admixtures, the mass loss of concrete under salt freeze-thaw cycles is slightly increased. At the same time, with regard to the relative dynamic modulus, the relative dynamic modulus of concrete with FA and BFS decreases more than that of the control concrete in the process of salt freeze-thaw cycles, while the three-mineral admixture concrete shows better salt freeze-thaw resistance than that of the control concrete.

The cumulative mass loss and the relative dynamic modulus with different air contents vary with salt freeze-thaw cycles show that the mass loss of concrete increases with the increase of salt freeze-thaw cycles, and the mass loss of concrete treated by AEA is significantly lower than that of control concrete. When the air content is in the range of 1%~6.5%, the mass loss of concrete will decrease with the increase of air content. When the air content of concrete is 2.5%, 4.5%, and 6.5%, with the increase of salt freeze-thaw cycles, the relative dynamic modulus of concrete is basically stable at 90%, while for the concrete without AEA, at 30 salt freeze-thaw cycles, the relative dynamic modulus has been reduced to 60%. It can be seen that in the appropriate range of air content, with the increase of air content, the number of tiny airtight bubbles in hardened concrete increases, which will greatly improve the salt freeze-thaw resistance of concrete [25, 31].

4. Conclusions

The mechanical properties, physical properties, and salt freeze-thaw resistance of concrete specimens were tested in this study. Based on the test results, the influences of mineral admixtures and different air contents on the mechanical properties, physical properties, and salt freeze-thaw

resistance of concrete were analyzed. The following conclusions could be reached:

(1) The mechanical properties of concrete decreased with the increase of FA content, while the mechanical properties tended to increase with the increase of BFS or SF content. The surface resistivity of concrete showed an increasing trend with the increase of FA, BFS, and SF content. The rapid chloride permeability gradually decreased with the increase of mineral admixture content.

(2) The salt freeze-thaw resistance of concrete decreased with the increase of FA content. However, the salt freeze-thaw resistance of concrete increased with the increase of BFS or SF. Especially, adding an appropriate amount of SF can significantly improve the salt freeze-thaw resistance of concrete.

(3) When adding 15% FA and 15% BFS, the mechanical properties, surface resistivity, and rapid chloride permeability of concrete will be improved, but the salt freeze-thaw resistance of concrete will decrease. When adding 15% FA, 15% BFS, and 6% SF, the mechanical properties, resistivity, and rapid chloride permeability of concrete will be greatly improved, and the salt freeze-thaw resistance of concrete will be slightly improved.

(4) Within the air content range of 1%~6.5%, as the air content increased, the compressive strength of concrete decreased, and the flexural strength first increased and then decreased. The surface resistivity of concrete increased with the increase of air content, and the rapid chloride permeability of concrete first decreased and then increased. The air content plays a major role in the salt freeze-thaw resistance of concrete, and the salt freeze-thaw resistance of concrete increased with the increase of air content.

(5) Surface resistivity of concrete has a good exponential function relationship with strength and a good power function relationship with rapid chloride permeability. Therefore, it is of great significance for engineering quality control to use the four-probe method to test surface resistivity. The strength and durability of concrete can be quickly and nondestructively estimated according to the regression equation.

Data Availability

The data used to support the findings of this study are available from the corresponding author upon request.

Conflicts of Interest

The authors declare that they have no conflicts of interest.

Acknowledgments

This research was funded by Nanning Excellent Young Scientist Program (grant number: RC20180108), Nanning Excellent Young Scientist Program and Guangxi Beibu Gulf Economic Zone Major Talent Program (grant number: RC20190206), Science and Technology Base and Talent Special Project of Guangxi Province (grant number: AD19245152), "Yongjiang Plan" of Nanning Leading Talents in Innovation and Entrepreneurship (grant number: 2018-01-04), and Scientific and Technological Project of Science and Technology Department of Jilin Province (grant number: 20190303052SF). This research was also supported by China Postdoctoral Science Foundation (grant number: 2021T140262).

References

[1] Y. B. Jiao, Y. Zhang, M. Guo, L. Zhang, H. Ning, and S. Liu, "Mechanical and fracture properties of ultra-high performance concrete (UHPC) containing waste glass sand as partial replacement material," *Journal of Cleaner Production*, vol. 277, Article ID 123501, 2020.

[2] C. S. Poon, S. C. Kou, and L. Lam, "Compressive strength, chloride diffusivity and pore structure of high performance metakaolin and silica fume concrete," *Construction and Building Materials*, vol. 20, no. 10, pp. 858–865, 2006.

[3] F. Pacheco-Torgal, Y. Ding, and S. Jalali, "Properties and durability of concrete containing polymeric wastes (tyre rubber and polyethylene terephthalate bottles): an overview," *Construction and Building Materials*, vol. 30, pp. 714–724, 2012.

[4] H. B. Liu, G. B. Luo, H. B. Wei, and H. Yu, "Strength, permeability, and freeze-thaw durability of pervious concrete with different aggregate sizes, porosities, and water-binder ratios," *Applied Sciences-Basel*, vol. 8, no. 8, p. 1217, 2018.

[5] G. Tan, Z. Zhu, W. Wang et al., "Flexural ductility and crack-controlling capacity of polypropylene fiber reinforced ECC thin sheet with waste superfine river sand based on acoustic emission analysis," *Construction and Building Materials*, vol. 277, Article ID 122321, 2021.

[6] X. J. Shi, P. Park, Y. Rew, K. Huang, and C. Sim, "Constitutive behaviors of steel fiber reinforced concrete under uniaxial compression and tension," *Construction and Building Materials*, vol. 233, Article ID 117316, 2020.

[7] W. S. Wang, Y. C. Cheng, and G. J. Tan, "Design optimization of SBS-modified asphalt mixture reinforced with eco-friendly basalt fiber based on response surface methodology," *Materials*, vol. 11, no. 8, 2018.

[8] K. Amini, P. Vosoughi, H. Ceylan, and P. Taylor, "Effect of mixture proportions on concrete performance," *Construction and Building Materials*, vol. 212, pp. 77–84, 2019.

[9] H. B. Liu, S. Q. Liu, P. L. Zhou, and Y. Zhang, "Mechanical properties and crack classification of basalt fiber RPC based on acoustic emission parameters," *Applied Sciences-Basel*, vol. 9, no. 18, p. 3931, 2019.

[10] W.-J. Long, K. H. Khayat, A. Yahia, and F. Xing, "Rheological approach in proportioning and evaluating prestressed self-consolidating concrete," *Cement and Concrete Composites*, vol. 82, pp. 105–116, 2017.

[11] X. Shi, A. Mukhopadhyay, D. Zollinger, and Z. Grasley, "Economic input-output life cycle assessment of concrete pavement containing recycled concrete aggregate," *Journal of Cleaner Production*, vol. 225, pp. 414–425, 2019.

[12] X. Shi, A. Mukhopadhyay, and K.-W. Liu, "Mix design formulation and evaluation of portland cement concrete paving

mixtures containing reclaimed asphalt pavement," *Construction and Building Materials*, vol. 152, pp. 756–768, 2017.
[13] H. J. Wu, Z. Diao, and K. Z. Fan, "Study on durability of non-dispersible concrete in seawater environment," *International Journal of Structural Integrity*, vol. 11, no. 3, pp. 443–452, 2020.
[14] N. Xie, M. Akin, and X. Shi, "Permeable concrete pavements: a review of environmental benefits and durability," *Journal of Cleaner Production*, vol. 210, pp. 1605–1621, 2019.
[15] G. Dimitriou, P. Savva, and M. F. Petrou, "Enhancing mechanical and durability properties of recycled aggregate concrete," *Construction and Building Materials*, vol. 158, pp. 228–235, 2018.
[16] H. B. Liu, G. B. Luo, Y. F. Gong, and H. B. Wei, "Mechanical properties, permeability, and freeze-thaw resistance of pervious concrete modified by waste crumb rubbers," *Applied Sciences-Basel*, vol. 8, no. 10, 2018.
[17] W. S. Wang, G. J. Tan, C. Y. Liang, Y. Wang, and Y. C. Cheng, "Study on viscoelastic properties of asphalt mixtures incorporating SBS polymer and basalt fiber under freeze-thaw cycles," *Polymers*, vol. 12, no. 8, p. 1804, 2020.
[18] N. Xie, X. M. Shi, and Y. Zhang, "Impacts of potassium acetate and sodium-chloride deicers on concrete," *Journal of Materials in Civil Engineering*, vol. 29, no. 3, 2017.
[19] Y. Farnam, M. Krafcik, L. Liston et al., "Evaluating the use of phase change materials in concrete pavement to melt ice and snow," *Journal of Materials in Civil Engineering*, vol. 28, no. 4, 2016.
[20] Z. Sun and G. W. Scherer, "Measurement and simulation of dendritic growth of ice in cement paste," *Cement and Concrete Research*, vol. 40, no. 9, pp. 1393–1402, 2010.
[21] J. Yuan, H. Lu, Q. B. Yang, and J. Ling, "Mechanisms on the salt-frost scaling of concrete," *Journal of Materials in Civil Engineering*, vol. 29, no. 3, 2017.
[22] B. Lei, W. Li, Z. Tang, V. W. Y. Tam, and Z. Sun, "Durability of recycled aggregate concrete under coupling mechanical loading and freeze-thaw cycle in salt-solution," *Construction and Building Materials*, vol. 163, pp. 840–849, 2018.
[23] Q. L. Guo, Q. Liu, P. Zhang et al., "Temperature and pressure dependent behaviors of moisture diffusion in dense asphalt mixture," *Construction and Building Materials*, vol. 246, Article ID 118500, 2020.
[24] Q. Guo, G. Li, Y. Gao et al., "Experimental investigation on bonding property of asphalt-aggregate interface under the actions of salt immersion and freeze-thaw cycles," *Construction and Building Materials*, vol. 206, pp. 590–599, 2019.
[25] G. J. Ke, J. Zhang, B. Tian, and J. Wang, "Characteristic analysis of concrete air entraining agents in different media," *Cement and Concrete Research*, vol. 135, Article ID 106142, 2020.
[26] F. Huang, H. Li, Z. Yi, Z. Wang, and Y. Xie, "The rheological properties of self-compacting concrete containing superplasticizer and air-entraining agent," *Construction and Building Materials*, vol. 166, pp. 833–838, 2018.
[27] D. M. Wellman, K. E. Parker, L. Powers et al., "Effect of iron and carbonation on the diffusion of iodine and rhenium in waste encasement concrete and soil fill material under hydraulically unsaturated conditions," *Applied Geochemistry*, vol. 23, no. 8, pp. 2256–2271, 2008.
[28] G. C. Shan, S. Zhao, M. Qiao, N. Gao, J. Chen, and Q. Ran, "Synergism effects of coconut diethanol amide and anionic surfactants for entraining stable air bubbles into concrete," *Construction and Building Materials*, vol. 237, Article ID 117625, 2020.
[29] M. Khoshroo, A. A. Shirzadi Javid, and A. Katebi, "Effect of chloride treatment curing condition on the mechanical properties and durability of concrete containing zeolite and micro-nano-bubble water," *Construction and Building Materials*, vol. 177, pp. 417–427, 2018.
[30] L. Du and K. J. Folliard, "Mechanisms of air entrainment in concrete," *Cement and Concrete Research*, vol. 35, no. 8, pp. 1463–1471, 2005.
[31] S. Chatterji, "Freezing of air-entrained cement-based materials and specific actions of air-entraining agents," *Cement and Concrete Composites*, vol. 25, no. 7, pp. 759–765, 2003.
[32] Z. Liu and W. Hansen, "Pore damage in cementitious binders caused by deicer salt frost exposure," *Construction and Building Materials*, vol. 98, pp. 204–216, 2015.
[33] J. Yuan, Z. Du, Y. Wu, and F. Xiao, "Freezing-thawing resistance evaluations of concrete pavements with deicing salts based on various surfaces and air void parameters," *Construction and Building Materials*, vol. 204, pp. 317–326, 2019.
[34] P. Duan, Z. Shui, W. Chen, and C. Shen, "Efficiency of mineral admixtures in concrete: microstructure, compressive strength and stability of hydrate phases," *Applied Clay Science*, vol. 83-84, pp. 115–121, 2013.
[35] H. B. Liu, G. B. Luo, L. H. Wang, and Y. Gong, "Strength time-varying and freeze-thaw durability of sustainable pervious concrete pavement material containing waste fly ash," *Sustainability*, vol. 11, no. 1, 2019.
[36] J. J. Valenza and G. W. Scherer, "Mechanism for salt scaling of a cementitious surface," *Materials and Structures*, vol. 40, no. 3, pp. 259–268, 2007.
[37] B. Amini and S. S. Tehrani, "Simultaneous effects of salted water and water flow on asphalt concrete pavement deterioration under freeze-thaw cycles," *International Journal of Pavement Engineering*, vol. 15, no. 5, pp. 383–391, 2014.
[38] S.-H. Han, "Influence of diffusion coefficient on chloride ion penetration of concrete structure," *Construction and Building Materials*, vol. 21, no. 2, pp. 370–378, 2007.
[39] Q. Yuan, D. Zhou, B. Li, H. Huang, and C. Shi, "Effect of mineral admixtures on the structural build-up of cement paste," *Construction and Building Materials*, vol. 160, pp. 117–126, 2018.
[40] C. Wu, L. Li, W. Wang, and Z. Gu, "Experimental characterization of viscoelastic behaviors of nano-TiO_2/$CaCo_3$ modified asphalt and asphalt mixture," *Nanomaterials*, vol. 11, no. 1, 2021.
[41] Y. Li, J. Bao, and Y. Guo, "The relationship between autogenous shrinkage and pore structure of cement paste with mineral admixtures," *Construction and Building Materials*, vol. 24, no. 10, pp. 1855–1860, 2010.
[42] W. Sun, Y. Zhang, S. Liu, and Y. Zhang, "The influence of mineral admixtures on resistance to corrosion of steel bars in green high-performance concrete," *Cement and Concrete Research*, vol. 34, no. 10, pp. 1781–1785, 2004.
[43] J. D. Bapat, "Performance of cement concrete with mineral admixtures," *Advances in Cement Research*, vol. 13, no. 4, pp. 139–155, 2001.
[44] C.-H. Lim, Y.-S. Yoon, and J.-H. Kim, "Genetic algorithm in mix proportioning of high-performance concrete," *Cement and Concrete Research*, vol. 34, no. 3, pp. 409–420, 2004.
[45] C. Liang, X. Xu, H. Chen et al., "Machine learning approach to develop a novel multi-objective optimization method for pavement material proportion," *Applied Sciences*, vol. 11, no. 2, 2021.
[46] M. Shahnewaz, R. Machial, M. S. Alam, and A. Rteil, "Optimized shear design equation for slender concrete beams reinforced with FRP bars and stirrups using genetic algorithm

and reliability analysis," *Engineering Structures*, vol. 107, pp. 151–165, 2016.

[47] S. Kim, H. B. Choi, Y. Shin, G.-H. Kim, and D.-S. Seo, "Optimizing the mixing proportion with neural networks based on genetic algorithms for recycled aggregate concrete," *Advances in Materials Science and Engineering*, vol. 2013, Article ID 527089, 10 pages, 2013.

[48] W. J. Park, T. Noguchi, and H. S. Lee, "Genetic algorithm in mix proportion design of recycled aggregate concrete," *Computers & concrete*, vol. 11, no. 3, pp. 183–199, 2013.

[49] H. Yazici, "The effect of silica fume and high-volume class c fly ash on mechanical properties, chloride penetration and freeze-thaw resistance of self-compacting concrete," *Construction and Building Materials*, vol. 22, no. 4, pp. 456–462, 2008.

[50] C.-W. Chung, C.-S. Shon, and Y.-S. Kim, "Chloride ion diffusivity of fly ash and silica fume concretes exposed to freeze-thaw cycles," *Construction and Building Materials*, vol. 24, no. 9, pp. 1739–1745, 2010.

[51] A. Mardani-Aghabaglou, G. İnan Sezer, and K. Ramyar, "Comparison of fly ash, silica fume and metakaolin from mechanical properties and durability performance of mortar mixtures view point," *Construction and Building Materials*, vol. 70, pp. 17–25, 2014.

[52] H. Ziari, P. Hayati, and J. Sobhani, "Airfield self-consolidating concrete pavements (ASCCP): mechanical and durability properties," *Construction and Building Materials*, vol. 72, pp. 174–181, 2014.

[53] M. J. Islam, M. S. Meherier, and A. K. M. R. Islam, "Effects of waste pet as coarse aggregate on the fresh and harden properties of concrete," *Construction and Building Materials*, vol. 125, pp. 946–951, 2016.

[54] W. S. Wang, Y. C. Cheng, H. P. Chen, and G. Tan, "Study on the performances of waste crumb rubber modified asphalt mixture with eco-friendly diatomite and basalt fiber," *Sustainability*, vol. 11, no. 19, 2019.

[55] Q. Guo, L. Li, Y. Cheng, Y. Jiao, and C. Xu, "Laboratory evaluation on performance of diatomite and glass fiber compound modified asphalt mixture," *Materials & Design (1980–2015)*, vol. 66, pp. 51–59, 2015.

[56] Q. L. Guo, H. Y. Wang, Y. Gao, Y. Jiao, F. Liu, and Z. Dong, "Investigation of the low-temperature properties and cracking resistance of fiber-reinforced asphalt concrete using the DIC technique," *Engineering Fracture Mechanics*, vol. 229, 2020.

[57] J. Tian, W. Wang, and Y. Du, "Damage behaviors of self-compacting concrete and prediction model under coupling effect of salt freeze-thaw and flexural load," *Construction and Building Materials*, vol. 119, pp. 241–250, 2016.

[58] M. An, Y. Wang, and Z. Yu, "Damage mechanisms of ultra-high-performance concrete under freeze-thaw cycling in salt solution considering the effect of rehydration," *Construction and Building Materials*, vol. 198, pp. 546–552, 2019.

[59] X. J. Li, W. S. Wang, Z. Q. Zhu, and K. Zhang, "Investigation on durability behaviour and optimization of concrete with triple-admixtures subjected to freeze-thaw cycles in salt solution," *Advances in Materials Science and Engineering*, vol. 2021, Article ID 5572011, 16 pages, 2021.

[60] A. Qi, X. H. Liu, Z. W. Wang, and Z. X. Chen, "Mechanical properties of the concrete containing ferronickel slag and blast furnace slag powder," *Construction and Building Materials*, vol. 231, Article ID 117120, 2020.

[61] H. B. Liu, G. B. Luo, L. H. Wang, W. Wang, W. Li, and Y. Gong, "Laboratory evaluation of eco-friendly pervious concrete pavement material containing silica fume," *Applied Sciences-Basel*, vol. 9, no. 1, p. 73, 2019.